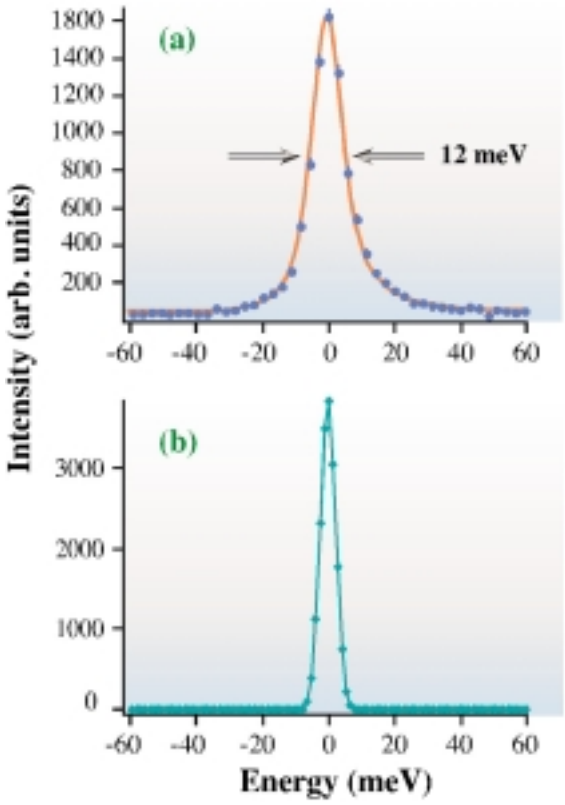

Fig. 3: ***(a)*** *Nuclear resonant quasi-elastic scattering from ^{57}Fe ions in Nafion.*
(b) *Nuclear resonant forward scattering from ^{57}Fe foil.*

OBSERVATION OF MAGNETIC RELAXATION IN AN $^{57}FeBO_3$ CRYSTAL BY USING NUCLEAR FORWARD SCATTERING

The Mössbauer time-domain spectroscopy using synchrotron radiation is suitable for the study of periodically perturbed nuclear resonant scattering. The time divided measurements are realized by phase-locking the periodic perturbation to the SR pulse. The quantum beats and dynamical beats give us information on the hyperfine interactions, the nuclear excited states and the motion of the resonant atom [1,2]. Recently, by applying the polarimetry technique, it has been shown that the oscillation of a hyperfine field on the plane perpendicular to the light axis can change the direction of the electric field vector of nuclear forward scattering (NFS) [3] (Figure 1).

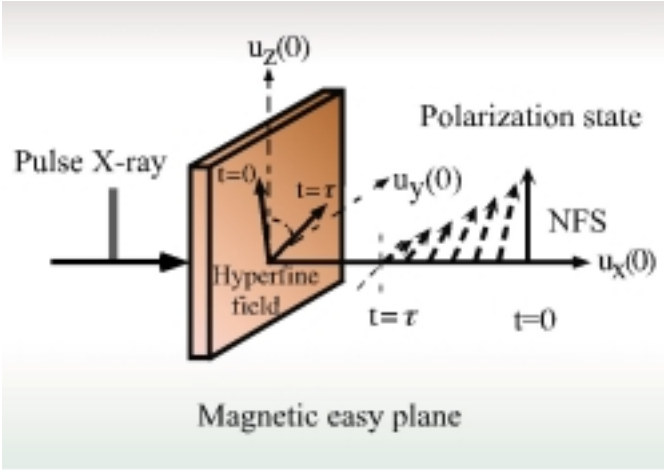

Fig. 1: Rotation of the polarization plane of NFS.

Makoto Seto[a], Rie Haruki[a] and Shinji Kitao[b]
(a) Kyoto University
(b) SPring-8 / JAERI

E-mail: seto@rri.kyoto-u.ac.jp

References

[1] M. Seto *et al., Phys. Rev. Lett.* **74** (1995) 3828.
[2] S. Kitao *et al.*, to be published in *Jpn. J. Appl. Phys. Suppl.*
[3] A. I. Chumakov *et al., Phys. Rev. B* **56** (1997) 10758.
[4] R. Haruki *et al.*, in preparation.

In the present study, we investigated the beam properties of NFS in the magnetic relaxation system of the $^{57}FeBO_3$ antiferromagnetic single crystal. The experiment was performed at the undulator beamline **BL09XU**. The storage ring was operated in 21-bunch mode at 20 mA. A SR pulse was emitted only at 228 ns intervals with a typically 50 ps width. The experimental setup is shown in Figure 2. The magnetic relaxation was caused by the fall-off of the external pulse magnetic field. Then, the

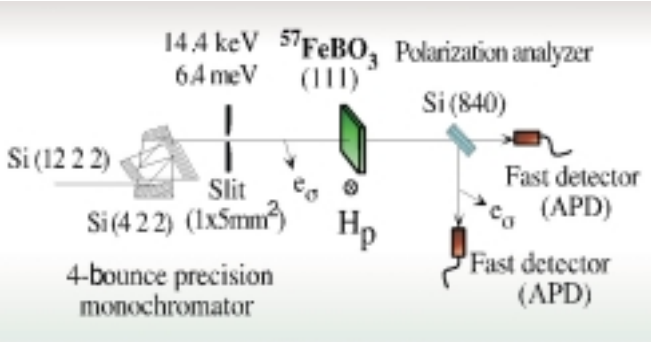

Fig. 2: Experimental setup.

magnetically unstable multidomain state (electron spin fluctuation system) was excited in the $^{57}FeBO_3$ single crystal over the magnetic relaxation time [4]. The magnetic field was phase-locked to the SR pulse signal. (Magnetic field parameters: strength 28 Oe, pulse width 80 ns, fall-off time 7 ns, frequency ~400 kHz.) The M ssbauer time spectra were measured with and without a Si(840) polarization analyzer crystal. (This crystal reflects only the s -polarized X-ray.) We measured eleven spectra at the intervals of 228 ns in the time range of 2.5 ms after the fall-off.

The normalized time spectra measured after 140 ns from the fall-off time are shown in Figure 3. From the comparison of plots (a) and (b) in Fig. 3, the intensity of the time spectrum with Si(840) is clearly lower.

This is explained as follows, at the instance of SR incidence after the fall-off time, NFS from the $^{57}FeBO_3$ crystal plate occurs with the σ -polarization as a result of nuclear transitions with $\Delta m = 0, -1$. Then, each magnetization (electron spin) vector in the multidomain of the crystal rotates randomly on the magnetic easy plane, $^{57}FeBO_3$ (111), due to the magnetic relaxation, and the hyperfine fields also rotate randomly. Therefore, the electric field vector of NFS is changed from the s -polarization to the mixed polarization. In our experimental arrangement, the π -polarized component of NFS cannot reach the detector in the case of using the analyzer crystal Si(840). As a result, the time spectra with Si(840) are reduced according to the mean velocity of the atomic spin rotation in the target material. A depolarization factor expressing the speed of the polarization mixing of NFS over the magnetic relaxation time, $\tilde{P}(t) = \tilde{I}^{\pi+\sigma}(t) - \tilde{I}^{\sigma}(t) / \tilde{I}^{\pi+\sigma}(t)$, was obtained from the time spectra with and without Si(840). Here, $\tilde{I}(t)$ is the normalized integrated intensity of the time spectra in the specific time range. The specific time ranges were set at 10~20 ns (fast rotation: This value is comparable to a nuclear Larmor precession time of $^{57}FeBO_3$ crystal) and 20~60 ns (slow rotation) in the time spectra. The corresponding parameter $\tilde{P}(t)$ of each time spectrum is shown in Figure 4. This figure indicates that, during 2.5 μs

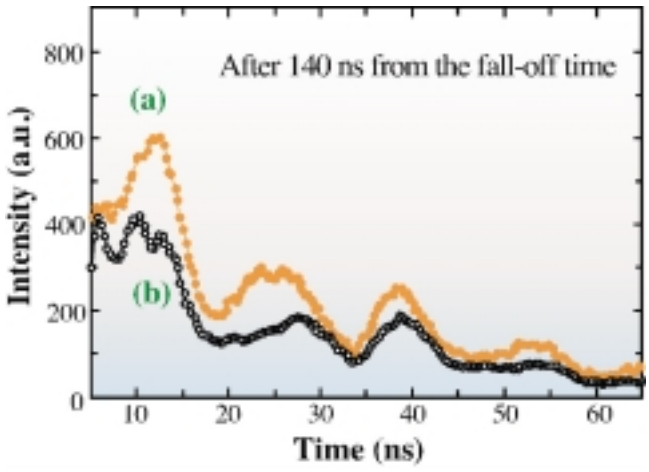

Fig. 3: Time spectra of the perturbed NFS.
***(a)** without and **(b)** with Si(840) polarization analyzer.*

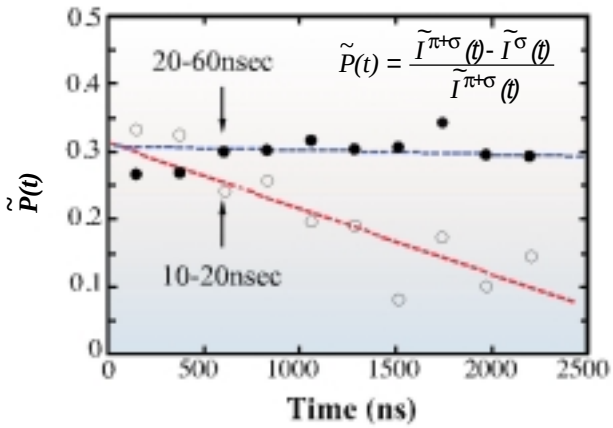

Fig. 4: Time dependent depolarization factor.

fall-off time, $\tilde{P}(t)_{10\sim20ns}$ shows a speedy reduction, whereas $\tilde{P}(t)_{10\sim60ns}$ keeps a nearly fixed value. Fluctuation of the magnetic moment in the crystal is decreased by the time development of the magnetic relaxation.

Takaya Mitsui
SPring-8 / JAERI

E-mail: taka@sp8sun.spring8.or.jp

References

[1] Yu.V. Shvyd'ko, *Hyp. Interact.* **90** (1994) 287.
[2] T. Mitsui *et al., Jpn. J. Appl. Phys.* **36** (1997) 6525.
[3] T. Mitsui *et al., Hyp. Interact.* (c) **3** (1998) 429.
[4] S. Kikuta, *Hyp. Interact.* **90** (1994) 335.

TIME AND ENERGY SPECTRA OF INTERNAL CONVERSION ELECTRONS FROM ^{57}Fe FOIL

Energy distribution and time spectra of internal conversion electrons from ^{57}Fe foil were measured at the **BL09XU** beamline. The emission signal of conversion electrons excited with incident X-ray photons was discriminated by electron energy analysis and intense prompt noise was excluded in the signal processing. The apparatus consists of an electrostatic electron energy analyzer and a sample manipulator contained in an ultrahigh vacuum chamber. The analyzer we developed was a planar electrostatic quadrupole type assembled on a 203 mm Conflat-type flange. The electrons incident through an entrance slit of the analyzer were deflected at an angle of 90˚ inside the hyperbolic electrostatic field. The acceptance angle and the energy resolution were 0.04 π and 4%, respectively.

An avalanche photodiode (APD) detector was attached at the exit of the analyzer. The APD detector proved high detection efficiency for high-energy electrons as well as excellent time response (< 1 ns) and noise characteristics (< 0.01 cps). The photons from an in-vacuum undulator are monochromatized to a band-width of 2 meV by a high-resolution nested channel-cut monochromator. The counting rate of APD detector for the prompt emission of photoelectrons was 1.4 x 10^6 cps. The energy spectrum of the electrons excited with a 14.413 keV X-ray is shown in Figure 1. To suppress the enormous counting rate of prompt emission of photoelectrons, the output pulse of the APD detector is discriminated in the time-domain between 10 and 190 ns after the incidence of synchrotron radiation. The peaks of K- and L-shell conversion electrons and KLL Auger electrons are clearly observed in the figure. The maximum counting rate at the peak energy of K-shell conversion electrons was 0.51 cps. The tail in the low energy side is due to the cascade inelastic scattering of electrons inside the sample. The energy resolution of 4% corresponds to the escape depth of 20 nm.

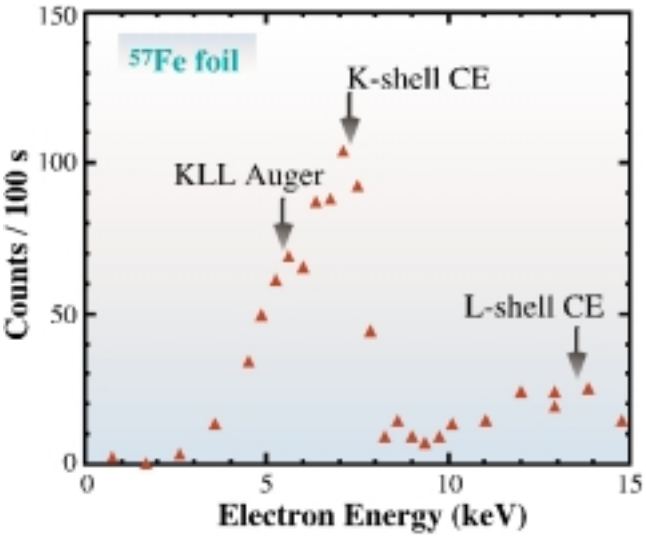

Fig.1: Energy distribution of electron emission from ^{57}Fe foil within a time-interval between 10 and 190 ns after incidence of primary photons.